Pulsating regime of magnetic deflagration in crystals of molecular magnets

M. Modestov, V. Bychkov, and M. Marklund
Department of Physics, Umeå University, SE-901 87 Umeå, Sweden
(Received 8 February 2011; revised manuscript received 18 April 2011; published 14 June 2011)

The stability of a magnetic deflagration front in a media of molecular magnets, such as Mn_{12} acetate, is considered. It is demonstrated that stationary deflagration is unstable with respect to one-dimensional perturbations if the energy barrier of the magnets is sufficiently high in comparison with the release of Zeeman energy at the front; their ratio may be interpreted as an analog to the Zeldovich number, as found in problems of combustion. When the Zeldovich number exceeds a certain critical value, a stationary deflagration front becomes unstable and propagates in a pulsating regime. Analytical estimates for the critical Zeldovich number are obtained. The linear stage of the instability is investigated numerically by solving the eigenvalue problem. The nonlinear stage is studied using direct numerical simulations. The parameter domain required for experimental observations of the pulsating regime is discussed.

DOI: 10.1103/PhysRevB.83.214417 PACS number(s): 75.50.Xx, 75.60.Jk, 47.70.Pq

I. INTRODUCTION

Molecular magnets have been a subject of intense experimental and theoretical studies for almost two decades (see Refs. 1 and 2 for a review). The field belongs to mesoscopic physics as typical length scales are between microscopic and macroscopic. Such an intermediate parameter regime provides unique conditions for observing quantum and classical phenomena acting together. Besides, a large magnetic spin of a single molecule makes molecular magnets natural candidates for novel magnetic storage media and quantum computing.[3,4]

Two prominent and well-investigated materials in this research field are Mn_{12} acetate and Fe_8, both demonstrating superparamagnetic properties.[1] They have a large spin at the ground state ($S = 10$) and strong magnetic anisotropy with ten pairs of degenerated levels corresponding to positive and negative projections S_z on a chosen axis, and an additional level with $S_z = 0$ (see Refs. 5–8). When an external magnetic field is applied to a sample of molecular magnets along the crystal axis, then spin orientation in the direction of the field becomes preferable. At low temperature all molecules populate only one level (e.g., $S_z = 10$) and the magnetization reaches the saturation value. If the direction of the external magnetic field changes to the opposite one, then the former ground state of the molecules becomes metastable with an increased potential energy (the Zeeman energy). An energy barrier hinders direct transition of the molecules from the metastable state to the new ground state, which, therefore, can occur as thermal relaxation or as avalanches. Thermal relaxation goes slowly and uniformly in space for the whole sample. At temperatures of a few Kelvin this process may be neglected, since its characteristic time is rather large, e.g., $\sim$2 months for Mn_{12} at 2 K.[5] However, many experimental works on molecular magnets demonstrated quite a fast transition in the form of an avalanche with a characteristic time of approximately a few milliseconds.[9,10] Recent detailed studies of the avalanche revealed that the spin reversal does not happen simultaneously within the whole sample in that case, but it occurs in a narrow zone propagating as a front with a velocity of several meters per second.[11–18] The avalanche is accompanied by a significant heat release, similar to a deflagration wave in combustion, and for this reason it was named "magnetic deflagration."

In slow combustion, the deflagration front corresponds to a thin zone of chemical reactions separating the cold fuel mixture and the hot burned products.[19] The released energy is transmitted to the cold fuel mixture due to thermal conduction; the temperature of the fuel mixture increases, which stimulates chemical reactions. The slow combustion front propagates in gaseous mixtures with a substantially subsonic velocity within the range from several centimeters to several meters per second.[19] Analogously, in magnetic deflagration, the energy of the chemical reactions is replaced by the Zeeman energy of the molecular magnets in an external magnetic field. The released energy is distributed to the neighboring layers by thermal conduction, which increases the temperature of the originally cold medium and leads to a much higher probability of spin transition. In recent studies, Garanin and Chudnovsky[12] developed a theoretical description of a planar stationary magnetic deflagration with a maximal possible release of the Zeeman energy. They referred to such a regime as "full burning," meaning that initially all the molecules had spin in one direction and at the final stage all the molecules changed their spin. Since then, a number of papers have been devoted to ignition techniques and speed measurements of the magnetic deflagration in Mn_{12}.[14–18] Magnetic avalanches have been also observed in other materials, such as the intermetallic compound Gd_5Ge_4.[20] However, it is not necessarily that all molecules participate in the avalanche. Due to the thermal equilibrium, a part of the molecules can occupy the other energy level with the opposite spin direction (see Fig. 1), hence only a part of molecules contributes to the total Zeeman energy. As we show in the present paper, the Zeeman energy release depends on the external magnetic field and on the initial concentration of the active molecules. A sufficiently low-energy release may lead to a pulsating regime of magnetic deflagration.

The aim of the present work is to study the stability of a planar stationary front of magnetic deflagration. Here, we demonstrate that stationary deflagration is unstable with respect to one-dimensional (1D) perturbations if the Zeeman energy release at the front is sufficiently low in comparison with the energy barrier of the spin transition. The condition of the instability may be formulated using the Zeldovich number, similar to the case of combustion of solid propellants.[19,21–25] In

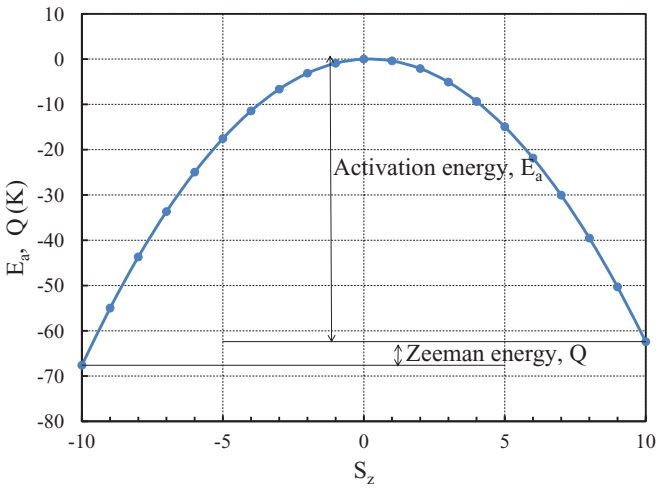

FIG. 1. (Color online) The energy levels for the magnetic molecule system of Mn_{12} in the external magnetic field $H_z = 0.2$ T.

the problem of magnetic deflagration, the Zeldovich number is essentially given by the ratio of the energy barrier of the molecular magnets and the temperature at the deflagration as determined by the Zeeman energy release. When the Zeldovich number exceeds a certain critical value, a stationary deflagration front becomes unstable and propagates in a pulsating regime. We obtain analytical estimates for the critical Zeldovich number. We investigate the linear stage of the instability numerically by solving the eigenvalue problem. We study the nonlinear stage using direct numerical simulations. We also discuss the experimental parameters required for observations of the pulsating regime.

II. A PLANAR STATIONARY FRONT WITH INCOMPLETE ZEEMAN ENERGY RELEASE

We consider a system of molecular magnets placed in an external magnetic field, taking Mn_{12} acetate as a particular example. The simplified Hamiltonian of the system has been suggested to take the form[12]

$$\mathcal{H} = -DS_z^2 - g\mu_B H_z S_z, \tag{1}$$

where S denotes the spin, $D \approx 0.65$ K is the magnetic anisotropy constant, $g \approx 1.94$ is the gyromagnetic factor, μ_B is the Bohr magneton, and H_z is the external magnetic field.

The energy levels for a molecule magnet Mn_{12} in the external field of $H_z = 0.2$ T are depicted in Fig. 1. In Fig. 1 we indicate the Zeeman energy Q and the energy barrier E_a of the transition from the metastable state to the ground state, which plays the role of the activation energy for magnetic deflagration (both values are presented in temperature units). Using the Hamiltonian Eq. (1) we find how these two energies depend on the magnetic field, according to

$$E_a = DS_z^2 - g\mu_B H_z S_z + \frac{g^2}{4D}\mu_B^2 H_z^2 \tag{2}$$

and

$$Q = 2g\mu_B H_z S_z. \tag{3}$$

The last term in Eq. (2) is quite small as compared to the first two terms, so the activation energy decreases with an increase of the magnetic field. However, the Zeeman energy increases linearly with the magnetic field. If the magnetic field is high enough, the energy difference between the ground state ($S_z = -10$) and the metastable state ($S_z = 10$) is rather large, so that *all* the molecules tend to occupy the lowest-energy level, i.e., $S_z = -10$ in Fig. 1. When the direction of the external magnetic field switches to the opposite one, then the ground state and the metastable state exchange places and *all* the molecules change their spin projection to the opposite one. Garanin and Chudnovsky identified such a transition as "full burning" of molecular magnets.[12] They also indicated that such a regime is possible if the magnetic field is stronger than a certain critical value. Still, the external magnetic field is a controlled parameter of the experiments, which allows reducing the energy difference between the stable and metastable levels in comparison with the equilibrium temperature.

In that case the Zeeman energy is rather low, and we obtain a considerable fraction of molecules on the first energy level according to

$$n = \frac{1}{\exp(Q/T) + 1}, \tag{4}$$

where the total number of molecules in all energy levels corresponds to unity. We stress that in our case the Zeeman energy can be comparable to or smaller than the final temperature, so that both terms in the denominator of Eq. (4) are important. In typical experimental conditions, the population of levels above the first one is negligible. At the same time, the fraction at the first level, Eq. (4), may be significant in a low magnetic field and cannot be neglected. As we will see, the stability of magnetic deflagration is sensitive to the activation energy scaled by the energy release in the process. This ratio increases also when the active Mn_{12} molecules are "diluted" with some neutral media, as it was performed experimentally in, e.g., Refs. 26–28. When mixed carefully with other compounds, the Mn_{12} molecules retain their magnetic properties. Since the heat release in magnetic deflagration happens only due to active magnet molecules, then the neutral compound reduces the total energy release and the final temperature of the sample T_f, thus increasing the scaled activation energy E_a/T_f. As a result, the scaled activation energy in magnetic deflagration becomes a parameter, which may be controlled in the experiments by the external magnetic field and by the level of dilution.

The governing equations for magnetic deflagration are[12]

$$\frac{\partial E}{\partial t} = \nabla \cdot (\kappa \nabla E) - fQ\frac{\partial n}{\partial t}, \tag{5}$$

$$\frac{\partial n}{\partial t} = -\frac{1}{\tau_R}\exp\left(-\frac{E_a}{T}\right)\left[n - \frac{1}{\exp(Q/T)+1}\right] \tag{6}$$

where E is the thermal phonon energy, κ is thermal diffusion of energy, Q is the Zeeman energy release in temperature units, $f \leqslant 1$ indicates possible reduction of the energy release because of dilution of active molecules ($f = 1$ corresponds to zero dilution), n is the fraction of magnetic molecules in the metastable state, E_a is the energy barrier of tunneling measured in temperature units, and τ_R is a constant of time

dimension. The parameter τ_R characterizes the time of the spin reversal with the common experimental evaluation $\tau_R \sim 10^{-7}$ (see Refs. 11–15). A more accurate value of τ_R may be obtained indirectly by measuring the deflagration speed and the activation energy, and using a numerical solution such as the one presented in this work. In general, τ_R may depend on temperature, but we take it to be constant because of the lack of experimental data on the subject. In magnetic deflagration, thermal diffusion and heat capacity depend strongly on temperature. Following Ref. 12, we take the heat capacity in the classical form corresponding to phonons,[29]

$$C = Ak_B \left(\frac{T}{\Theta_D}\right)^{\alpha}, \tag{7}$$

where Θ_D is the Debye temperature, with $\Theta_D = 38$ K for Mn_{12}, k_B is the Boltzmann constant, $A = 12\pi^4/5$ corresponds to the simple crystal model, and α is the problem dimension [we take $\alpha = 3$, which corresponds to the three-dimensional (3D) geometry]. The dependence of thermal diffusion on temperature may be taken in the form $\kappa \propto T^{-\beta}$, where parameter β was considered in Refs. 12 and 30 within the range between 0 and 13/3. In the present paper we take $\beta = 3$; variations of this parameter change the deflagration structure in the preheating zone, but they have a minor influence on the deflagration stability. Using the definition of heat capacity $C = dE/dT$, we find the phonon energy as a function of temperature,

$$E = \frac{Ak_B}{\alpha+1}\left(\frac{T}{\Theta_D}\right)^{\alpha} T. \tag{8}$$

An important parameter of deflagration dynamics is determined by the ratio of the energy barrier (in temperature units) and the temperature in the hot region E_a/T_f. A combustion counterpart of this value is related to the activation energy of the chemical reaction, which is typically rather large. In the case of complete burning in magnetic deflagration of Mn_{12}, this parameter was evaluated in Ref. 12 as $E_a/T_f \approx 6$, which is not a large value. At the same time, this parameter may increase almost without limits at low magnetic fields and for considerable dilution of active molecular magnets. When the ratio E_a/T_f is very large, the transition from the metastable to stable states goes in a thin region. In a general case of finite E_a/T_f, Eqs. (5) and (6) may be solved numerically as an eigenvalue problem.

First, we calculate the final temperature in the hot region behind the magnetic deflagration front. Using the energy conservation and Eqs. (4), (5), and (8), we obtain

$$\frac{AT_0^{\alpha+1}}{(\alpha+1)\Theta_D^{\alpha}} + fQ\left(1 - \frac{1}{\exp(Q/T_0)+1}\right) = \frac{AT_f^{\alpha+1}}{(\alpha+1)\Theta_D^{\alpha}} + \frac{fQ}{\exp(Q/T_f)+1}. \tag{9}$$

Equation (9) determines the final temperature T_f as a function of the magnetic field, the dilution factor f, and other parameters of the process. The first terms on both sides of Eq. (9) stand for the thermal energy, though the initial thermal energy is small and usually can be neglected. The other terms indicate the Zeeman energy due to the fractions of molecules with a corresponding spin direction. In the present work, both

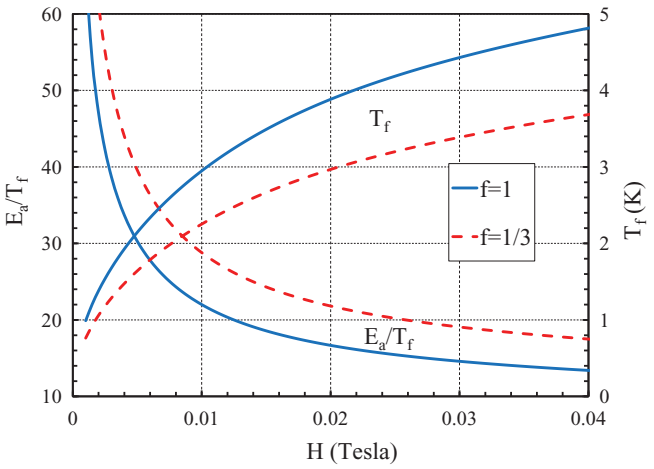

FIG. 2. (Color online) The final temperature and the scaled activation energy in magnetic deflagration vs the magnetic field for the initial temperature $T_0 = 0.2$ K and two dilution factors $f = 1, 1/3$.

Zeeman terms are comparable by order of magnitude; their balance yields the final thermal energy and Eq. (9) requires a numerical solution. This is different from the simplified case considered in Ref. 12. As we pointed out above, Ref. 12 studied the case of all molecules changing the spin projection, e.g., from $S_z = -10$ to 10. In that case Eq. (9) reduces to $fQ(\alpha+1)\Theta_D^{\alpha} = AT_f^{\alpha+1}$ and may be solved analytically. In Fig. 2 we show the numerical solution to Eq. (9), i.e., the final temperature and the scaled activation energy versus the magnetic field for two dilution factors $f = 1, 1/3$. In Fig. 2 we take the initial temperature $T_0 = 0.2$ K, though it has minor influence on the result. The dilution factor $f = 1$ stands for pure Mn_{12} media, while $f = 1/3$ means that the average energy release is three times lower in comparison with the pure substance. The final temperature increases with the magnetic field, while the scaled activation energy decreases. The change in the scaled activation energy due to the dilution factor may be also considerable.

We consider a stationary solution to Eqs. (5) and (6) in the form of a planar front propagating with velocity U_f. To be particular, we assume that the front moves along the x axis in the negative direction, as shown in Fig. 3. Taking the reference frame of the front, we find

$$U_f \frac{d}{dx}(E + fQn) = \frac{d}{dx}\left(\kappa \frac{dE}{dx}\right), \tag{10}$$

$$U_f \frac{dn}{dx} = -\frac{1}{\tau_R}\exp\left(-\frac{E_a}{T}\right)\left[n - \frac{1}{\exp(Q/T)+1}\right]. \tag{11}$$

In the limit of a large activation energy $E_a/T_f \gg 1$, the transition region may be presented as a surface of weak discontinuity, where energy and temperature are continuous and tend to their maximal values $E \to E_f$, $T \to T_f(E_f)$, while their derivatives experience a jump. In this limit one obtains the magnetic deflagration velocity[19]

$$U_f = \sqrt{\frac{\kappa_f}{Z\tau_R}}\exp\left(-\frac{E_a}{2T_f}\right), \tag{12}$$

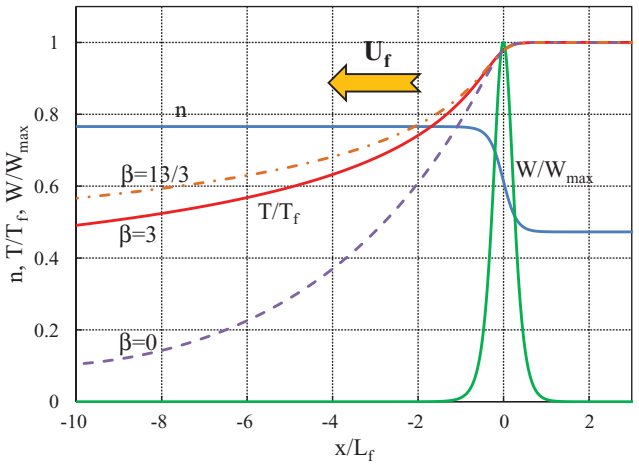

FIG. 3. (Color online) Stationary profiles of concentration, temperature, and energy release. The plot parameters are $E_a/T_f = 30$, $\beta = 3$, $\theta_0 = 0.2$. The dashed and dashed-dotted lines show the respective temperature profiles for $\beta = 0, 13/3$.

where

$$Z = \frac{E_a}{T_f}\frac{fQ(n_f - n_0)}{C_f T_f} = \frac{1}{(\alpha+1)}\frac{E_a}{T_f} \tag{13}$$

plays the role of the Zeldovich number; the last relation in Eq. (13) follows from Eqs. (7), (8), and (10). Equation (12) for the deflagration velocity coincides with Eq. (109) in Ref. 12. Equation (12) provides implicit dependence of the front velocity on the magnetic field, as the activation energy, final temperature, and the Zeldovich number are also functions of the magnetic field. Experimentally, the dependence has been demonstrated and discussed in several papers.[11,13–15] With the accuracy of a factor of $1/(\alpha+1)$, the Zeldovich number shows the ratio of the activation energy and the final temperature in the deflagration front. We can find the dependence of the Zeldovich number upon the main experimental parameters of the problem, taking into account Eqs. (2), (3), (7), (8), and (10):

$$Z = \left[\frac{A}{2(\alpha+1)^{\alpha+2}\Theta_D^{\alpha} g\mu_B S_z H_z f(n_0 - n_f)}\right]^{\frac{1}{\alpha+1}} \times \left(DS_z^2 - g\mu_B H_z S_z + \frac{g^2}{4D}\mu_B^2 H_z^2\right). \tag{14}$$

Equation (14) shows how the Zeldovich number depends on the magnetic field and the dilution factor. In particular, high values of the Zeldovich number correspond to the low-field strength. For a simplified quantitative estimate one can neglect the magnetic terms in the second pair of parentheses, which provide a contribution of less than a few percent for fields ~0.1 T and smaller, and find an evaluation for the Zeldovich number

$$Z \approx 1.3[H_z f(n_0 - n_f)]^{-1/4}, \tag{15}$$

where H_z is the magnetic field in Tesla.

III. ANALYTICAL ESTIMATES FOR THE PULSATION INSTABILITY

In this section we obtain an analytical scaling for the 1D instability of the magnetic deflagration front in the model of a thin transition zone, i.e., at a large Zeldovich number $Z \gg 1$. In that case, according to Eq. (12), the deflagration velocity is extremely sensitive to temperature variations in the transition zone. In comparison with the Arrhenius function $\exp(-E_a/2T_f)$, all other parameters in Eq. (12) may be treated as constant. The temperature in the transition zone may vary because of the front perturbations, and the instant front velocity may be written as

$$U_t = U_f \exp\left(\frac{E_a}{2T_f} - \frac{E_a}{2T_t}\right), \tag{16}$$

where label f refers to the stationary case, while t indicates the time-dependent temperature in the infinitely thin transition zone. The position of the transition zone $x = \phi(t)$ in the stationary reference frame is determined by the equation

$$\frac{\partial\phi}{\partial t} = -U_f\left[\exp\left(\frac{E_a}{2T_f} - \frac{E_a}{2T_t}\right) - 1\right], \tag{17}$$

where the first minus sign indicates propagation of the front in the negative direction. The boundary conditions at the transition region may be found to be similar to Refs. 19 and 22. Integrating Eq. (5) twice over the transitional zone, we obtain continuous energy and temperature,

$$E_{\phi+} = E_{\phi-}, \tag{18}$$

where the labels ϕ_+ and ϕ_- correspond to the hot and cold sides of the transition zone, respectively. The first derivative of energy (i.e., energy flux) experiences a jump at the interface as

$$-U_f Q n_0 \exp\left(\frac{E_a}{2T_f} - \frac{E_a}{2T_t}\right) = \kappa_f\left(\frac{\partial E}{\partial x}\right)_{\phi+} - \kappa_f\left(\frac{\partial E}{\partial x}\right)_{\phi-}. \tag{19}$$

We investigate the linear stability of the stationary deflagration and consider small perturbations of all variables in the exponential form $\tilde{E} \propto \exp(\sigma t)$, where the growth rate σ may have both real and imaginary parts. We solve the stability problem analytically in the limit of a thin transition zone similar to Ref. 19. Outside the transition zone the perturbed equations (5) and (6) are

$$\sigma\tilde{E} + U_f\frac{\partial\tilde{E}}{\partial x} = \frac{\partial^2}{\partial x^2}(\kappa\tilde{E}), \tag{20}$$

$$\sigma\tilde{n} + U_f\frac{\partial\tilde{n}}{\partial x} = 0. \tag{21}$$

Behind the transition zone we have $\tilde{n} = 0$. First we consider a hypothetical case of a constant coefficient of thermal conduction $\kappa = \text{const} = \kappa_f$. Solving Eq. (20) outside the

transition zone with $\tilde{E} \propto \exp(\mu x)$, we find two modes,

$$\mu^2 - \frac{U_f}{\kappa_f}\mu - \frac{\sigma}{\kappa_f} = 0, \tag{22}$$

$$\mu_\pm = \frac{U_f}{2\kappa_f} \mp \sqrt{\frac{U_f^2}{4\kappa_f^2} + \frac{\sigma}{\kappa_f}}, \tag{23}$$

with labels + and − indicating media behind and ahead of the transition zone. In the case of magnetic deflagration, thermal conduction decreases strongly with temperature $\kappa \propto T^{-\beta}$. Still, the mode behind the transition zone with $\mu_+ < 0$ is an exact solution even in that case, since the temperature behind the transition zone is uniform in the stationary deflagration. On the contrary, the mode ahead of the transition zone with $\mu_- > 0$ is only an approximation. Similar to the combustion theory,[19] we may define the parameter $L_f \equiv \kappa_f / U_f$ as the deflagration front thickness related to thermal conduction in the hot region. At the same time, the characteristic length scale of the temperature profile in the stationary deflagration increases in the cold layers as $\kappa(T)/U_f$, which allows to consider them as quasiuniform with respect to the perturbations. Indeed, the mode ahead of the transition zone describes the decay of perturbations at the length scale μ_-^{-1} with

$$\mu_- = \frac{1}{2L_f}[1 + \sqrt{1 + 4\sigma L_f/U_f}] \propto \frac{1}{L_f}. \tag{24}$$

Therefore, investigating the 1D instability analytically, it is justified to consider only the heating layer of the size approximately L_f close to the transition zone and to treat the coefficient of thermal conduction as approximately constant. The numerical solution to the problem obtained below supports the analytical approximation.

We consider perturbations of the boundary conditions (17)–(19) at the transition surface, following the analysis of Chap. 4 in Ref. 19. After heavy but straightforward algebra we end up with a simple quadratic equation,

$$\left(\frac{4\sigma L}{U_f}\right)^2 - \frac{4\sigma L}{U_f}(Z^2/4 - 2Z - 1) + 2Z = 0, \tag{25}$$

which is similar to the respective result in the combustion theory.[19] Equation (25) describes the instability growth rate as a function of the Zeldovich number. According to Eq. (25), the instability develops for $Z > 4 + 2\sqrt{5} \approx 8.5$. Close to this critical value the real part of the growth rate $\mathrm{Re}\,\sigma$ goes to zero, while the imaginary part remains finite, $\omega = \mathrm{Im}\,\sigma \neq 0$, which indicates the pulsation regime of the instability. The obtained critical value of the Zeldovich number corresponds to rather high scaled activation energy $E_a/T_f \approx 34$ [see Eq. (13)], in comparison with the values typical for the regime of all molecules participating in the avalanche.[12] Still, this value is attainable experimentally for smaller magnetic fields and some dilution of the active molecules. At an even larger value of the Zeldovich number, $Z = 11.7$, corresponding to $E_a/T_f = 46.8$, Eq. (25) demonstrates bifurcation, so that the instability growth rate becomes purely real with zero imaginary part for $Z > 11.7$. Below we will compare the analytical scaling Eq. (25) to the numerical solution to the problem, taking into account a finite width of the transition zone.

IV. NUMERICAL SOLUTION TO THE STABILITY PROBLEM, TAKING INTO ACCOUNT A FINITE WIDTH OF THE TRANSITION ZONE

In this section we solve the stability problem numerically, taking into account a finite width of the transition zone. We introduce dimensionless variables and parameters,

$$\theta = T/T_f, \quad a = n/n_0, \quad \xi = x/L_f,$$

$$\Theta = E_a/T_f, \quad \Delta = Q/T_f, \quad \kappa = \kappa_f \theta^{-\beta} \tag{26}$$

and rewrite the evolution equations (5) and (6) as

$$\theta^\alpha \frac{\partial\theta}{\partial\tau} + \theta^\alpha \frac{\partial\theta}{\partial\xi} = \frac{\partial}{\partial\xi}\left(\theta^{\alpha-\beta}\frac{\partial\theta}{\partial\xi}\right) + J\Lambda \exp\left(-\frac{\Theta}{\theta}\right) \times \left[a - \frac{1}{\exp(\Delta/\theta) + 1}\right], \tag{27}$$

$$\frac{\partial a}{\partial\tau} + \frac{\partial a}{\partial\xi} = -\Lambda \exp\left(-\frac{\Theta}{\theta}\right)\left[a - \frac{1}{\exp(\Delta/\theta) + 1}\right], \tag{28}$$

where $\Lambda = L_f/(\tau_R U_f)$ is an eigenvalue of the stationary problem and the designation J corresponds to the ratio of Zeeman and thermal energies,

$$J = \frac{f Q \Theta_D^\alpha}{A k_B T_f^{\alpha+1}}. \tag{29}$$

It can be shown that the parameter J is almost a constant, $J \approx 1/(\alpha + 1)$. We also introduce the thermal flux $\psi = \theta^{\alpha-\beta}\partial\theta/\partial\xi$, so that the stationary deflagration is described by the system of equations

$$\begin{aligned} \frac{\partial\psi}{\partial\xi} &= \theta^\beta\psi - J\Lambda a \exp\left(-\frac{\Theta}{\theta}\right), \\ \frac{\partial\theta}{\partial\xi} &= \theta^{\beta-\alpha}\psi, \\ \frac{\partial a}{\partial\xi} &= -\Lambda a \exp\left(-\frac{\Theta}{\theta}\right). \end{aligned} \tag{30}$$

The boundary conditions for the system (30) are obtained from a numerical solution to Eq. (9), which yields the final temperature and the concentration values. We integrate this system from the right-hand side (for the geometry of Fig. 3), starting with $\theta = 1$ and concentration a_f, and finish our integration when the concentration approaches asymptotically the value a_0; the scaled concentrations are determined by Eq. (4) for a fixed initial temperature. Typical profiles of scaled concentration, temperature, and energy release,

$$W = \Lambda \exp\left(-\frac{\Theta}{\theta}\right)\left\{a - \left[\exp\left(\frac{\Delta}{\theta}\right) + 1\right]^{-1}\right\}, \tag{31}$$

are depicted in Fig. 3 for the magnetic deflagration propagating to the left-hand side with $\beta = 3$. In Fig. 3, the scaled activation energy is taken rather high, $\Theta = 30$. The dashed and dashed-dotted lines show how the preheating zone depends on the parameter β. The front velocity is determined by the eigenvalue of the problem Λ in Eq. (30), which was computed numerically using the shooting method similar to Ref. 31. We can see in Fig. 3 that the final number of molecules in the metastable state behind the deflagration front is different from zero $n_f = 0.47$,

which indicates that burning is incomplete. The initial number of molecules in the metastable state is also different from unity, $n_0 = 0.77$, due to the nonzero temperature ahead of the front before switching of the magnetic field [see Eq. (4)]. Figure 3 shows also that the total thickness of the deflagration front is much larger than L_f. This difference in the characteristic length scales should be attributed, first of all, to the temperature dependence of thermal conduction. Still, even in the case of constant thermal conduction typically used in combustion problems, the effective flame thickness is almost an order of magnitude larger than the conventional definition for L_f, e.g., see Ref. 32.

Now we consider the stability of the magnetic deflagration. We investigate the dynamics of small perturbations of the stationary solution, so that all variables may be presented as $\varphi = \varphi_0 + \tilde{\varphi}\exp(\gamma\tau)$. Then the perturbed system (30) is

$$\frac{\partial\tilde{\psi}}{\partial\xi} = \theta^{\beta}\tilde{\psi} + (\theta^{\alpha}\gamma + \beta\theta^{\beta-1}\psi - JG)\tilde{\theta} - J\Lambda\exp\left(-\frac{\Theta}{\theta}\right)\tilde{a},$$
$$\frac{\partial\tilde{\theta}}{\partial\xi} = \theta^{\beta-\alpha}\tilde{\psi} + (\beta-\alpha)\,\theta^{\beta-\alpha-1}\psi\tilde{\theta},$$
$$\frac{\partial\tilde{a}}{\partial\xi} = -G\tilde{\theta} - \left[\gamma + \Lambda\exp\left(-\frac{\Theta}{\theta}\right)\right]\tilde{a}, \qquad (32)$$

where the designation

$$G = \Lambda\exp\left(-\frac{\Theta}{\theta}\right)\frac{1}{\theta^2}\left[\Theta a - \left(\Theta - \frac{\Delta}{\exp(\Delta/\theta)+1}\right)\times\frac{1}{\exp(\Delta/\theta)+1}\right]$$

has been introduced for brevity. Parameter γ stands for the scaled instability growth rate $\gamma = \sigma L_f/U_f$. In order to specify boundary conditions for the numerical solution, we find the decaying perturbation modes in the uniform regions $\tilde{\varphi} \propto \tilde{\varphi}\exp(\mu\xi)$. The system (32) involves three modes in the uniform regions: two in the hot matter with $\mu < 0$, $\xi \to +\infty$, and one in the cold matter with $\mu > 0$, $\xi \to -\infty$. We integrate the system (32) numerically three times, corresponding to the three perturbation modes: once from the left-hand (cold) side and twice from the right-hand (hot) side. At some point, e.g., at the maximum of the energy release, the solutions form a matrix, with the determinant depending on the instability growth rate γ. The condition of the zero matrix determinant specifies the growth rate γ as an eigenvalue of the system (32). This method has been applied successfully in studies of different hydrodynamic instabilities, e.g., the Rayleigh-Taylor instability and the Darrieus-Landau instability of combustion and laser ablation, as well as for other plasma instabilities.[31,33–35]

V. RESULTS AND DISCUSSIONS

A numerical solution to the stability problem is shown in Fig. 4 for different values of the scaled activation energy proportional to the Zeldovich number as $E_a/T_f = 4Z$ for a 3D problem; other deflagration parameters are the same as those used in Fig. 3. As we can see in Fig. 4, planar stationary magnetic deflagration is unstable at sufficiently large values of the scaled activation energy; the stability limit was calculated

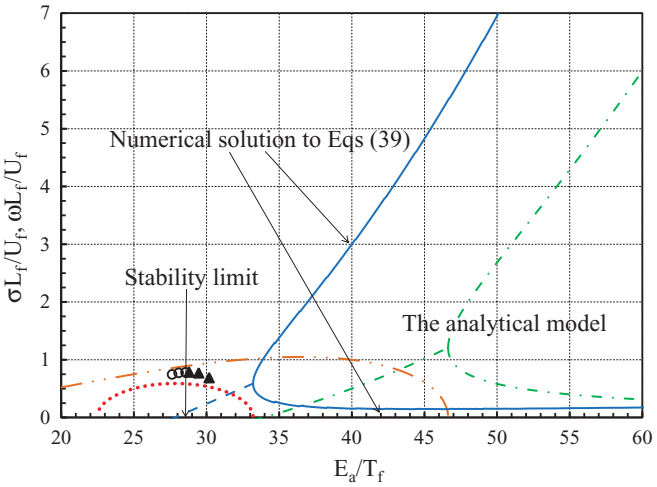

FIG. 4. (Color online) The instability growth rate σ and the perturbation frequency ω vs the scaled activation energy calculated for the same parameters as in Fig. 3. The solid lines show the domain of zero frequency; the dashed and dotted lines correspond to the regimes when perturbations have both a real (growth rate σ) and an imaginary part (frequency ω) in the problem eigenvalue. The dashed-dotted lines present the analytical model, Eq. (25). The markers show the results of the direct numerical simulations: the open circles stand for a stable region and the filled triangles represent the unstable pulsating regime of the deflagration.

as $E_a/T_f = 28.2$. The instability domain consists of two parts separated by a bifurcation point at $E_a/T_f = 33.2$. Most of the domain (to the right-hand side of the bifurcation point) corresponds to purely real instability growth rate $\sigma > 0$, with two branches describing the fast and slow perturbation modes (shown by the solid lines). The instability growth rate of the fast mode increases with the scaled activation energy without any limit. The analytical model, Eq. (25), predicts the asymptotic increase of the growth rate for the fast mode as $\sigma \propto (E_a/T_f)^2$ for $E_a/T_f \to \infty$. The growth rate of the slow mode decreases with the scaled activation energy. For this reason it is expected that the slow mode plays a noticeable role only close to the bifurcation point, where the growth rates of the fast and slow modes are comparable. In a small part of the instability domain, for intermediate values of the scaled activation energy in between the stability limit and the bifurcation point, $28.2 < E_a/T_f < 33.2$, the instability growth rate is complex with the real part $\sigma > 0$ (dashed line) and imaginary part ω (dotted line). Although this part of the instability domain is rather small, it indicates the physical outcome of the instability at the nonlinear stage. Because of the nonzero frequency $\omega \neq 0$, it is natural to expect that the instability leads to a pulsating regime of magnetic deflagration at the nonlinear stage. The analytical solution, Eq. (25), obtained within the model of a thin transition zone (dashed-dotted lines) shows qualitatively the same stability properties of magnetic deflagration as the numerical solution. Still, we observe a minor quantitative difference between the analytical model and the numerical solution. According to the analytical model, the stability limit and the bifurcation point are expected at $E_a/T_f = 34.0$ and $E_a/T_f = 46.8$, which differ by ~20%–30% from the respective numerical values.

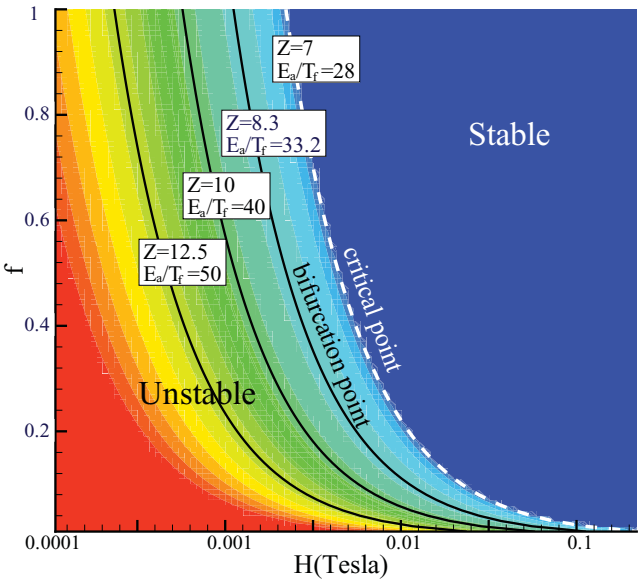

FIG. 5. (Color online) The stability limit (dashed line) of the magnetic deflagration in coordinates of the dilution factor f and the magnetic field H. The shading shows the instability growth rate. Other solid lines correspond to the respective constant values of the Zeldovich number.

The limited accuracy of the analytical model is due to the simplifying approximations of a constant coefficient of energy diffusion and an infinitely thin zone of energy release. In particular, the shortcomings of the discontinuity model have been discussed in Refs. 24 and 25 in the context of solid propellant combustion.

The numerical solution to the stability problem indicates the experimental parameters required to observe the unstable nonstationary regime of magnetic deflagration. We plot the stability diagram in Fig. 5 in f-H_z coordinates using Eq. (15); the shading represents absolute value of the instability growth rate. The dashed white line in Fig. 5 corresponds to the critical value of the Zeldovich number (the stability limit) obtained numerically. Magnetic deflagration propagates stationary in the parameter domain to the right-hand side of the stability limit, in the region of a high magnetic field. To the left-hand side of the critical curve, for a low magnetic field, the stationary magnetic deflagration is unstable, and we expect a pulsating regime of the deflagration front. Particularly, in the case of Mn_{12} with a dilution level $f = 1/3$, one should expect instability for magnetic fields below 10^{-2} T, which is possible to achieve experimentally.

In order to understand front dynamics at the nonlinear stage of the instability, we perform direct numerical simulation of Eqs. (27) and (28). In our simulations we use the method of finite difference for the spatial derivatives and the common fourth-order Runge-Kutta method for the time step integration. The results of our simulations, i.e., evolution of the magnetic deflagration speed, are shown in Fig. 6 for different values of the scaled activation energy. Figures 6(a) and 6(b) demonstrate front behavior close to the stability limit in the stable (a) and unstable (b) parameter domain. In the first case with $E_a/T_f = 28.55$, the velocity perturbation oscillates and decays in time, which implies a negative instability growth rate. On the

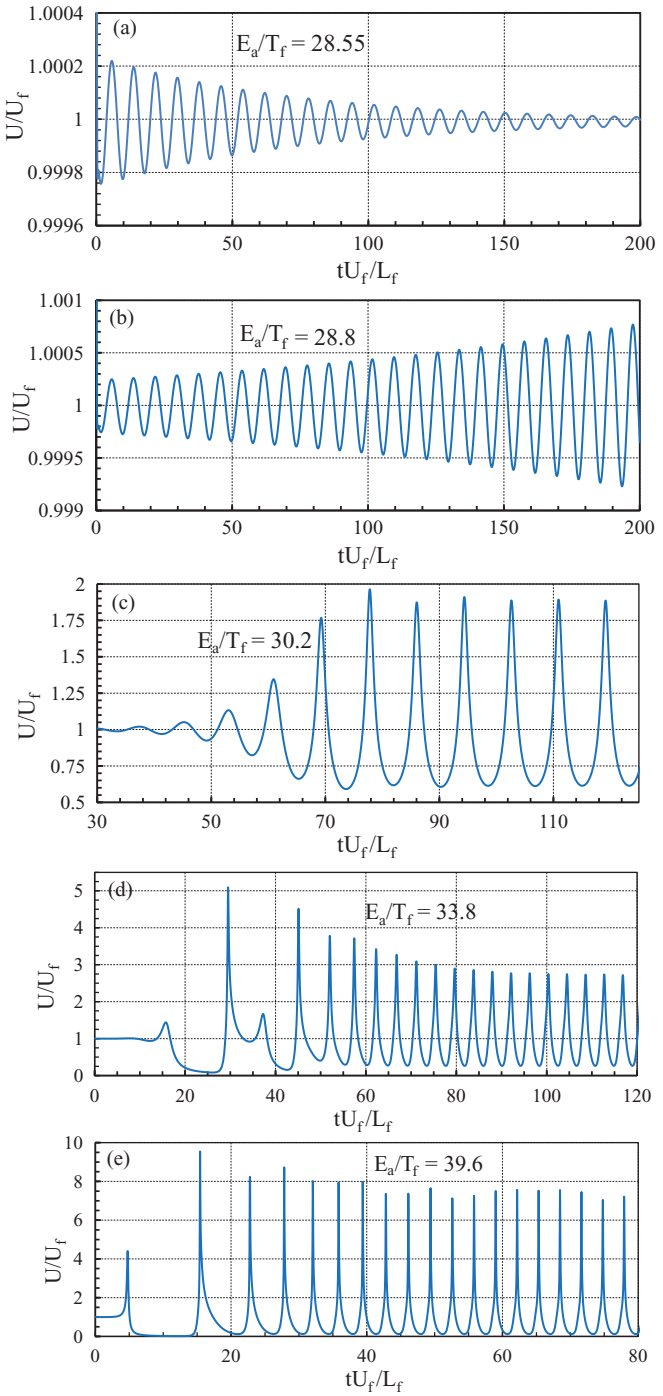

FIG. 6. (Color online) Deflagration speed vs time for different values of the scaled activation energy $E_a/T_f = 28.55$, 28.8, 30.2, 33.8, 39.6 for (a)–(e), respectively.

contrary, in Fig. 6(b) with $E_a/T_f = 28.8$, the amplitude of velocity oscillations grows with time, which corresponds to the instability onset. The markers in Fig. 4 show the oscillation frequency of the magnetic deflagration obtained in direct numerical simulations, with open circles and filled triangles standing for the stable and unstable regimes, respectively. As we can see, the direct numerical simulations are in good agreement with the solution to the eigenvalue problem,

which concerns both the stability limits and the oscillation frequency. Still, the instability is rather weak in Fig. 6(b), with the oscillations described well by the sine function. The nonlinear effects become noticeable for higher values of the scaled activation energy with sharp peaks and smooth troughs in the oscillations, as presented in Fig. 6(c) for $E_a/T_f = 30.2$. The simulations explain the physical mechanism of the obtained instability. Magnetic deflagration propagates due to two effects: release of the Zeeman energy in a thin transition zone and transfer of the energy to the cold layers (preheating) due to thermal conduction. In a stationary regime of magnetic deflagration, these two processes work at the same rate and balance each other. However, at high values of the activation energy, the rate of energy release is too sensitive to temperature in the transition zone. Small temperature perturbations may increase the rate of spin switching considerably, which makes the transition zone sweep fast over the preheated matter until it comes to cold regions and stops waiting for a new portion of cold matter to be preheated. As soon as it happens, the next pulsation of the front takes place.

It is interesting that Figs. 6(a)– 6(c) demonstrate three qualitatively different regimes of magnetic deflagration, although the activation energy changes only within 5% from Fig. 6(a) to Fig. 6(c). In Fig. 6(d) we take the activation energy $E_a/T_f = 33.8$ close to the bifurcation point and see a complicated front behavior at the onset of the velocity pulsations. Presumably, the complicated behavior happens because of two unstable modes with close instability growth rates at the vicinity of the bifurcation point. Still, after an initial transition period, the front pulsations resemble those of Fig. 6(c). Finally, taking an activation energy that is noticeably larger than the bifurcation point $E_a/T_f = 39.6$, we observe even more pronounced nonlinear features in the front oscillations, with even sharper peaks of large amplitude, as shown in Fig. 6(e). The obtained results are qualitatively similar to the pulsation instability of solid propellant combustion studied in, e.g., Refs. 21 and 23. Thus, the scaled activation energy (or the Zeldovich number) is the main parameter, which controls 1D stability properties of magnetic deflagration. Other problem parameters, the power exponents α, β, and the scaled initial temperature θ_0, influence the front stability slightly, as long as the Zeldovich number is fixed in agreement with the theoretical model of Sec. III.

VI. SUMMARY

In this paper we have obtained 1D instability of magnetic deflagration in a medium of molecular magnets. The main parameter of the problem is the Zeldovich number, which represents the activation energy of the system (in temperature units) scaled by the temperature at the deflagration front with a numerical factor depending on the type of heat capacity. We have demonstrated that the deflagration front becomes unstable when the Zeldovich number exceeds a certain critical value $Z \approx 7$. We have obtained analytical scaling for the instability parameters at a linear stage within the model of an infinitely thin zone of Zeeman energy release. We have also solved the eigenvalue stability problem numerically, taking into account the internal structure of the deflagration front. The numerical solution determines the experimental parameters necessary to observe the instability. Besides, we have performed direct numerical simulations, which demonstrated that the instability leads to a pulsating regime of magnetic deflagration at the nonlinear stage.

Although the present analysis is limited to the 1D case, it is known from combustion science that the pulsating instability may develop in 2D and 3D geometries as well,[19] producing a variety of nonlinear regimes, e.g., see recent experiments on gaseous combustion.[36] Reproducing these regimes for magnetic deflagration requires heavy 3D simulations, taking into account anisotropic properties of the crystals of molecule magnets, which is beyond the scope of the present work.

ACKNOWLEDGMENTS

The authors are grateful to Petter Minnhagen for useful discussions. This work was supported by the Swedish Research Council and by the Kempe Foundation.

[1] D. Gatteschi and R. Sessoli, Angew. Chem. Int. Ed. **42**, 268 (2003).
[2] E. del Barco, A. D. Kent, S. Hill, J. M. North, N. S. Dalal, E. Rumberger, D. N. Hendrikson, N. Chakov, and G. Christou, J. Low Temp. Phys. **140**, 119 (2005).
[3] M. N. Leuenberger and D. Loss, Nature (London) **410**, 789 (2001).
[4] J. Tejada, E. M. Chudnovsky, E. del Barco, J. M. Hernandez, and T. P. Spiller, Nanotechnology **12**, 181 (2001).
[5] R. Sessoli, D. Gatteschi, A. Caneschi, and M. A. Novak, Nature (London) **365**, 141 (1993).
[6] C. Paulsen, J.-G. Park, B. Barbara, R. Sessoli, and A. Caneschi, J. Magn. Magn. Mater. **140**, 1891 (1995).
[7] J. R. Friedman, M. P. Sarachik, J. Tejada, and R. Ziolo, Phys. Rev. Lett. **76**, 3830 (1996).
[8] L. Thomas, F. Lionti, R. Ballou, D. Gatteschi, R. Sessoli, and B. Barbara, Nature (London) **383**, 145 (1996).
[9] F. Fominaya, J. Villain, P. Gandit, J. Chaussy, and A. Caneschi, Phys. Rev. Lett. **79**, 1126 (1997).
[10] E. del Barco, J. M. Hernandez, M. Sales, J. Tejada, H. Rakoto, J. M. Broto, and E. M. Chudnovsky, Phys. Rev. B **60**, 11898 (1999).
[11] Y. Suzuki, M. P. Sarachik, E. M. Chudnovsky, S. McHugh, R. Gonzalez-Rubio, N. Avraham, Y. Myasoedov, E. Zeldov, H. Shtrikman, N. E. Chakov, and G. Christou, Phys. Rev. Lett. **95**, 147201 (2005).
[12] D. A. Garanin and E. M. Chudnovsky, Phys. Rev. B **76**, 054410 (2007).

[13] A. Hernandez-Minguez, J. M. Hernandez, F. Macia, A. Garcia-Santiago, J. Tejada, and P. V. Santos, Phys. Rev. Lett. **95**, 217205 (2005).
[14] S. McHugh, R. Jaafar, M. P. Sarachik, Y. Myasoedov, A. Finkler, H. Shtrikman, E. Zeldov, R. Bagai, and G. Christou, Phys. Rev. B **76**, 172410 (2007).
[15] A. Hernandez-Minguez, F. Macia, J. M. Hernandez, J. Tejada, and P. V. Santos, J. Magn. Magn. Mater. **320**, 1457 (2008).
[16] D. Villuendas, D. Gheorghe, A. Hernandez-Minguez, F. Macia, J. M. Hernandez, J. Tejada, and R. J. Wijngaarden, Europhys. Lett. **84**, 67010 (2008).
[17] S. McHugh, B. Wen, X. Ma, M. P. Sarachik, Y. Myasoedov, E. Zeldov, R. Bagai, and G. Christou, Phys. Rev. B **79**, 174413 (2009).
[18] W. Decelle, J. Vanacken, V. V. Moshchalkov, J. Tejada, J. M. Hernandez, and F. Macia, Phys. Rev. Lett. **102**, 027203 (2009).
[19] Ya. B. Zeldovich, G. I. Barenblatt, V. B. Librovich, and G. M. Makhviladze, *The Mathematical Theory of Combustion and Explosion* (Consultants Bureau, New York, 1985).
[20] S. Velez, J. M. Hernandez, A. Fernandez, F. Macia, C. Magen, P. A. Algarabel, J. Tejada, and E. M. Chudnovsky, Phys. Rev. B **81**, 064437 (2010).
[21] K. G. Shkadinsky, B. I. Khaikin, and A. G. Merzhanov, Combust. Explos. Shock Waves **7**, 15 (1971).
[22] B. J. Matkovsky and G. I. Sivashinsky, SIAM J. Appl. Math. **35**, 465 (1978).
[23] M. Frankel, V. Roytburd, and G. Sivashinsky, SIAM J. Appl. Math. **54**, 1101 (1994).
[24] V. V. Bychkov and M. A. Liberman, Phys. Rev. Lett. **73**, 1998 (1994).
[25] V. V. Bychkov and M. A. Liberman, Phys. Rep. **325**, 115 (2000).
[26] P. Artus, C. Boskovic, J. Yoo, W. E. Streib, L. C. Brunel, D. N. Hendrickson, and G. Christou, Inorg. Chem. **40**, 4199 (2001).
[27] C. Schlegel, J. van Slageren, M. Manoli, E. K. Brechin, and M. Dressel, Polyhedron **28**, 1834 (2009).
[28] T. L. Makarova, V. S. Zagaynova, and N. G. Spitsina, Phys. Status Solidi B **247**, 3018 (2010).
[29] C. Kittel, *Quantum Theory of Solids* (Wiley, New York, 1963).
[30] D. A. Garanin and V. S. Lutovinov, Ann. Phys. (NY) **218**, 293 (1992).
[31] M. Modestov, V. Bychkov, D. Valiev, and M. Marklund, Phys. Rev. E **80**, 046403 (2009).
[32] V. Akkerman, V. Bychkov, A. Petchenko, and L. E. Eriksson, Combust. Flame **145**, 675 (2006).
[33] O. Travnikov, V. Bychkov, and M. Liberman, Phys. Fluids **11**, 2657 (1999).
[34] M. Modestov, V. Bychkov, and M. Marklund, Phys. Plasmas **16**, 032106 (2009).
[35] V. Bychkov, M. Modestov, and M. Marklund, Phys. Plasmas **17**, 112107 (2010).
[36] G. Jomaas and C. K. Law, Phys. Fluids **22**, 124102 (2010).